P10R.13 WAVEFORM DESIGN FOR CASA X-BAND RADARS

Nitin Bharadwaj* and V. Chandrasekar
Colorado State University, Fort Collins, Colorado

1. INTRODUCTION

The Center for Collaborative Adaptive Sensing of the Atmosphere (CASA), an engineering research center established by the National Science Foundation (NSF) will deploy its first generation network of four low-power, short-range, X-band, dual-polarized Doppler weather radars known as NETRAD. Doppler weather radars transmitting pulses with uniform pulse repetition frequency (PRF) have a fundamental limitation on maximum unambiguous range (r_{max}) and maximum unambiguous velocity (v_{max}) given by

$$r_{max} v_{max} = \frac{c\lambda}{8} \qquad (1)$$

In (1) λ is radar wavelength and *c* is the velocity of light. The $r_{max} v_{max}$ limit reduces by a factor of three when the wavelength is changed from S-band to X-band. There is always a trade off between r_{max} and v_{max} (Range-velocity ambiguity). Precipitation particles can be distributed over a large area and the dynamic range of the radar reflectivity can be as high as 65 dB resulting in range overlay. Velocity measurements can span 100 m/s in severe storms resulting in velocity folding. NETRAD is primarily for "targeted applications" such as tornado detection, flash flood monitoring, and hydrological applications. Such applications will have range overlay and velocity folding problems with conventional pulse-pair processing. A testbed of smaller X-band radar systems is being developed within the ERC (Junyent et al. 2005). Figure 1 shows the range-velocity limitation of an X-band radar compared to S-band radar. X-band radars have a low unambiguous velocity due to their short wavelength, and increasing the PRF will result in multiple trip overlays as storms can extend over a large distance. It can be observed that range-velocity ambiguity is more severe for X-band radars compared to the conventional S band. For example, a commonly used one millisecond PRT results in an unambiguous velocity of 7.5 m/s. Several range-velocity ambiguity mitigation schemes have been proposed in the past. Staggered pulse-repetition-time (PRT) pulsing can be used to increase the unambiguous velocity (Zrnic and Mahapatra 1985), and Golestani et al. (1995) extends this concept for dual-polarized radars. Random phase coding of the transmitted pulse was proposed in Siggia (1983) to mitigate range overlay, and a systematic phase code and associated processing was suggested in Sachidananda and Zrnic (1999). A systematic phase code has been known to give better performance than random phase codes but requires a phase controlled amplifier klystron, traveling wave tube (TWT) or solid-state transmitter. All the above methods have been tested with S-band and C-band radars. This paper will describe the adaptive pulsing schemes for the individual radar nodes based on NETRAD operational requirements such as scan speeds, volume coverage pattern and system/hardware limitations to resolve range and velocity ambiguities. The pulsing schemes considered here will include phase coding and multi-PRF waveforms for X-band implementation. The advent of high-speed digital processor with IF sampling and extensive computational power with the ability of real time spectral processing makes such schemes possible.

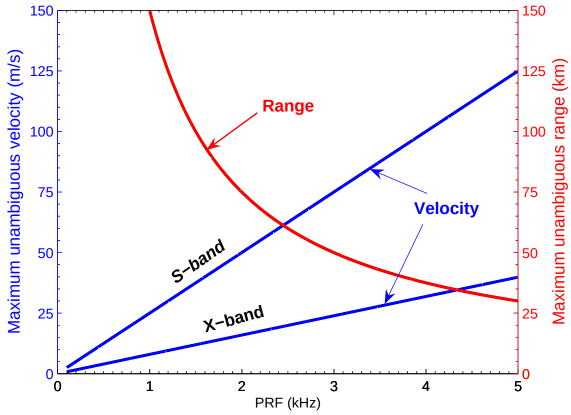

Figure 1: Comparisons of range-velocity limitations for S-band and X-band radars

2. DESIGN CONSIDERATIONS

The number of waveforms for the radar is constrained by the limitation of the hardware and system requirements.

*Corresponding author address: Nitin Bharadwaj, Colorado State University, Fort Collins, CO 80523
email : nitin@engr.colostate.edu

2.1. *Hardware Limitations*

The first generation CASA radar system are magnetron based systems with limited agility on duty cycle and supported waveforms. Junyent et al. (2005) gives a complete description of the radar system along with its features. The transmitter can deliver a maximum peak power of 25 kW at a duty cycle of 0.1%. The CASA radars operate at a range resolution of 100 m. Hence only a PRF of 1.5 kHz can be used at the peak power of 25 kW. The transmitter can be tuned below its maximum peak power allowing one to increase the duty cycle, which is used to accommodate the higher dual PRF bursts.For example, a 3 dB reduction in peak power will enable the transmitter to pulse at a PRF of 3 kHz. In addition there is a limitation on the ability to phase code the transmit pulses. Random phase coding is the only scheme that can be implemented. This is because a magnetron based system has a random start-up phase.

2.2. *Operation Requirements*

One of the main goals of NETRAD is to detect precursors to severe weather events. The feature identification of such events drives the scan strategies. For example, the volume coverage pattern (VCP) for feature identification and anticipation requires a volume scan with at least 13 tilts in $360°$ scans in about 3 minutes. Such scan strategies place limitations on the PRF and dwell times. In a NETRAD environment multiple radars will operate in a coordinated scanning mode. The captured features of the weather event are used to generate new radar scan strategies. The dwell time and PRF are directly related to the scan speeds and has to be adaptively changed based on the feature of the weather event. The meteorological commmand and control (MC&C) sends out the scan strategies to the individual radar sites where they are instantiated to a new volume coverage pattern.

3. Ground Clutter Filtering

Ground clutter is the radar return from non-meteorological targets that bias the reflectivity and velocity estimates. Ground clutter has a significant impact on the accuracy of radar parameters. Ground clutter filtering is performed by applying a notch filter centered at zero Doppler velocity. Elliptic filter have been traditionally used for clutter filtering. The advent of high speed digital processors enables clutter filtering in spectral domain. Siggia and Passarelli (2004) suggest an adaptive filtering technique called Gaussian Model Adaptive Processing (GMAP) wherein the clutter spectral coefficients are notched with a spectral clipper using a Gaussian model for the clutter spectral density. A Gaussian weather spectral density is recursively fit to the remaining points and the notched spectral coefficients are interpolated with the model. GMAP requires an *a priori* knowledge of the clutter spectral width and actually performs notch filtering. A similar spectral approach where a bimodal spectral fit (BSF) for clutter filtering is considered. The clutter contaminated weather echo can be modeled with a bimodal spectral distribution given by

$$S_m(\mu) = \frac{S_{0c}}{\sqrt{2\pi\sigma_c^2}} exp\{-\frac{v_k^2}{2\sigma_c^2}\} + \frac{S_0}{\sqrt{2\pi\sigma_v^2}} exp\{-\frac{(v_k - v_m)^2}{2\sigma_v^2}\} + N \quad (2)$$

where $\mu = [S_{0c}, \sigma_c, S_0, v_m, \sigma_v, N]^T$ with the subscripts "c" indicating clutter parameters and N is the noise power density. If S_x is the Doppler spectrum of the received signal then the bimodal spectral fit is obtained by solving the nonlinear optimization problem

$$\hat{\mu} = \arg\min_{\mu} E(S_x - S_m)^2 \quad (3)$$

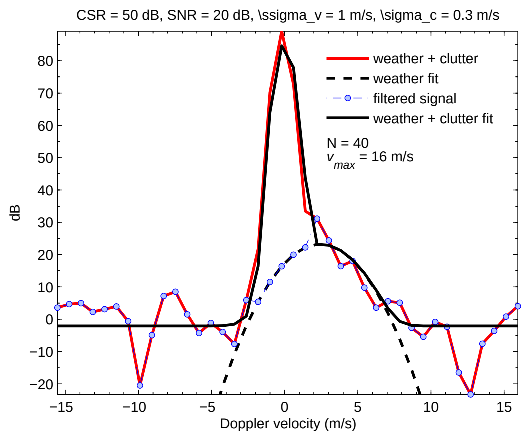

Figure 2: Clutter filtering with bimodal spectral distribution fits

Figure 2 illustrates the clutter filtering process for clutter-to-signal ratio (CSR) of 50 dB (CSR is a measure of the clutter suppression ability). Elements of μ corresponding to the weather return are used to replace the clutter spectral coefficients. The standard deviation, bias in reflectivity and velocity are shown in Fig. 3 and Fig. 4 respectively for a weather signal with $\sigma_v = 1$ m/s , $N = 40$ and a CSR of 50 dB. It can be seen that the bias in reflectivity is less than 1 dB for Doppler velocities greater than 4 m/s. The bias in reflectivity for Doppler velocities less than 4 m/s is high since $\sigma_v = 1$ m/s , however the bias is reduced for larger spectral widths as shown in

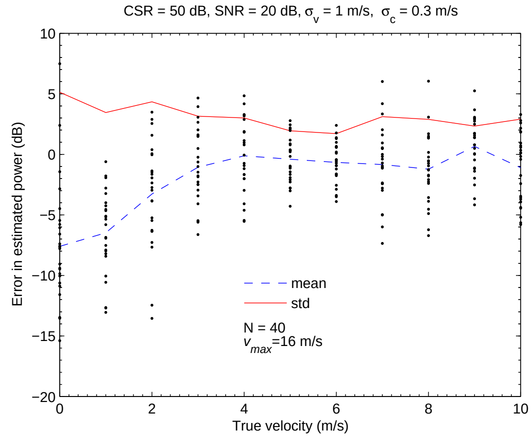

Figure 3: Bias and standard deviation of power after ground clutter filtering

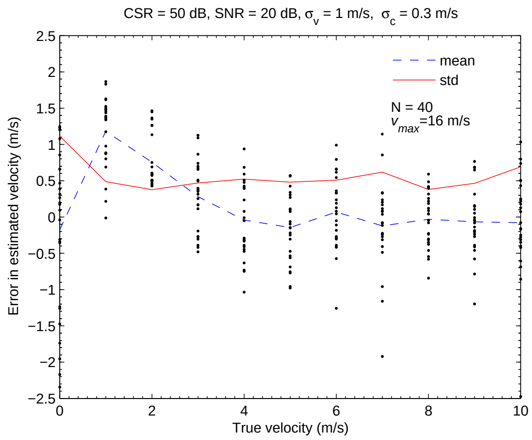

Figure 4: Bias and standard deviation of velocity after ground clutter filtering

Fig.5. The bias and standard deviation of velocity as a function of spectral width is shown in Fig.6. Since V_{max} is only 16 m/s the bias in velocity increases for $\sigma_v > 4$ m/s. The clutter suppression ability is limited by the number of pulses in a dwell time. The accuracy of velocity estimates degrade for lower PRF with $N < 40$.

4. Waveform Selection

A family of waveforms exist that can operate within the constraints imposed by the hardware limitations and the user requirements. The maximum PRF is limited by the duty cycle to 3 kHz. The minimum number of pulses at a given PRF is limited by the clutter suppression ability and the maximum is limited by the dwell time and thus the scan rate. Since the CASA radars has a beam width

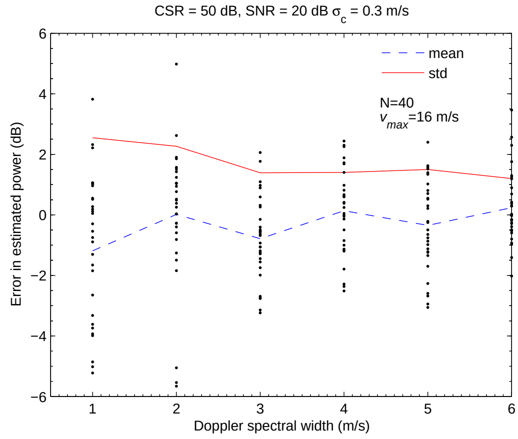

Figure 5: Bias and standard deviation of power after ground clutter filtering as a function of Doppler spectral width

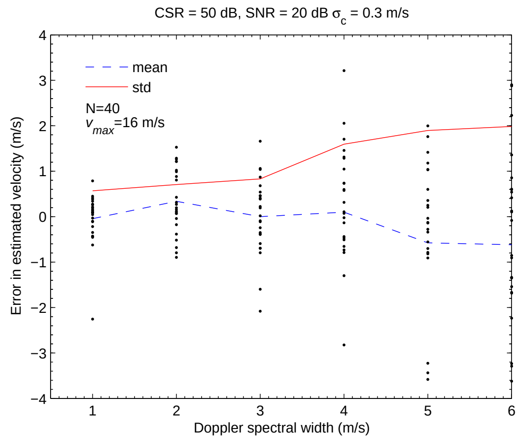

Figure 6: Bias and standard deviation of velocity after ground clutter filtering as a function of Doppler spectral width

of 2° the dwell time is made equal to the time taken by the main beam to move 1°. Based on the scan speed a different waveform is selected from a look-up table as shown in Fig.7. Since random phase coding occurs naturally in a magnetron based system random phase processing (Siggia 1983) will be performed. The region of recovery for the weak trip echo is determined by the strong trip parameters and the PRF. The standard deviation of the weak trip velocity estimate as a function of overlay power ratio and strong trip spectral width for a weak trip spectral width, $w_2 = 2$ m/s is shown in Fig.8. The solid white line indicates the recovery region for the weak trip (Sachidananda and Zrnic 1999).

Dual-PRF technique for extending the unambiguous velocity has been known for more than two decades

Scan Speed (deg/s)	PRF_1 (kHz)	PRF_2 (kHz)	~Velocity (m/s)	N_1	N_2
10~20	1.6 ~ 2.0	2.4 ~ 3.0	35 ~ 47	40 ~	54 ~
21	1.60	2.40	35.00	40	54
	1.70	2.55	40.00	42	58
	1.80	2.70	43.00	44	62
	1.90	2.85	45.00	46	66
	2.00	3.00	47.00	48	70
			Dual-PRF with phase coding		
Scan Speed (deg/s)	PRF_1 (kHz)	PRF_2 (kHz)	~Velocity (m/s)	N_1	N_2
22.00	3.00	~	23.90	136	~
25.00	3.00	~	23.90	120	~
28.00	3.00	~	23.90	107	~
31.00	3.00	~	23.90	96	~
34.00	3.00	~	23.90	88	~
37.00	3.00	~	23.90	81	~
40.00	3.00	~	23.90	75	~
43.00	3.00	~	23.90	69	~
46.00	3.00	~	23.90	65	~
49.00	3.00	~	23.90	61	~
52.00	3.00	~	23.90	57	~
55.00	3.00	~	23.90	54	~
Scan Speed (deg/s)	PRF_1 (kHz)	PRF_2 (kHz)	~Velocity (m/s)	N_1	N_2
55.00	3.00	~	23.90	54	~
58.00	3.00	~	23.90	51	~
61.00	3.00	~	23.90	49	~
64.00	3.00	~	23.90	46	~
67.00	3.00	~	23.90	44	~
70.00	3.00	~	23.90	42	~
73.00	3.00	~	23.90	41	~
			Single PRF without phase coding		

Figure 7: Number of pulses and PRF based on scan speeds

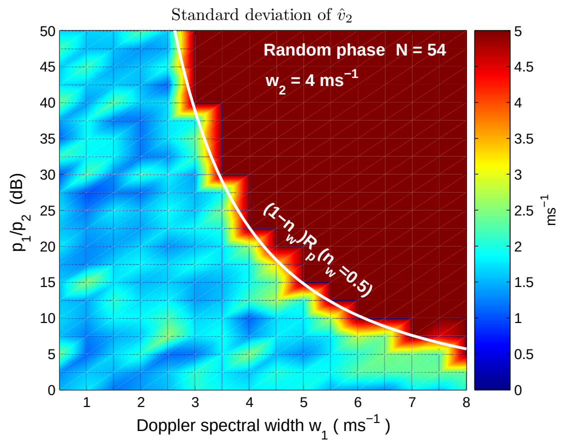

Figure 8: Standard deviation of weak trip velocity after random phase processing with PRF=3 kHz

and are available on many operational Doppler weather radars, especially shorter wavelength radar systems. Dual-PRF velocity estimates have higher standard deviations and hence, its only used to correct the original

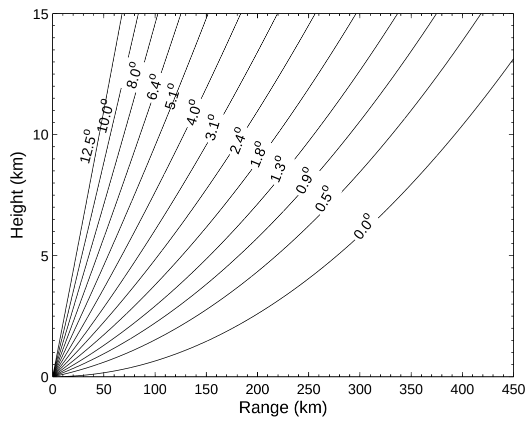

Figure 9: The height of the radar beam center as a function of elevation and range

folded velocity. The unfolding is performed by comparing the difference in the two velocity estimates corresponding to the two PRFs. However, there are unfolding errors that occur due to the inherent uncertainty in the folded velocity estimates. These unfolding errors can be corrected during post processing. An implementation of dual-PRF on an airborne weather radar at X-band is presented by Jorgensen et al. (2000) along with the analysis of unfolding errors. Since the higher PRF signal can be easily contaminated by second trip echoes random phase processing is performed on the higher PRF signal.

The exact waveform is selected from this table according to the volume coverage pattern determined by the MC&C. For example, consider a VCP with 13 tilts (Fig.9) in $360°$ scans in 3.5 minutes. A dual-PRF waveform with $PRF_1 = 2$ kHz and $PRF_2 = 3$ kHz with N=54 pulse each will able to provide a maximum unambiguous velocity of 47 m/s. A pulsing scheme with dual-PRF is illustrated in Fig.10 and Fig.11 shows a scatter plot of the true velocity versus the unfolded velocity obtained from random phase processing with dual-PRF. The unambiguous velocity is extended to more than 40 m/s while the overlay protection can be extended to 100km depending on the overlay conditions.

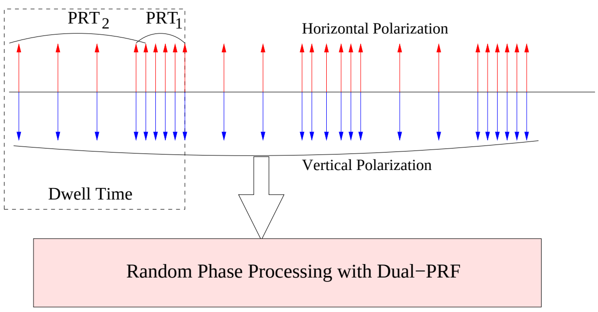

Figure 10: Staggered pulsing with random phase processing

5. Summary

The combination of smaller wavelength, low cost hardware and adaptive scan strategy enforce a stringent constraint on the waveform to mitigate range-velocity ambiguities. The waveform is chosen from a look-up table based on the adaptive scanning strategy. A bimodal spectral fit(BSF)is used for clutter filtering. A clutter suppression ratio of 50 dB is achieved with adequate performance in bias and accuracy. A dual-PRF waveform with

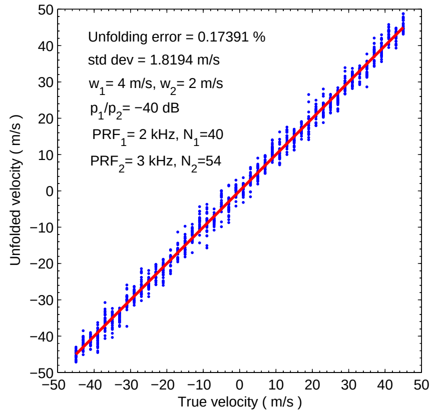

Figure 11: Scatter plot of true vs unfolded velocity with $PRF_1 = 2$ kHz and random phase processing with $PRF_2 = 3$ kHz

random phase coding for a VCP with 13 tilts provides a maximum unambiguous velocity of 47 m/s.

Acknowledgement This work is supported by the Engineering Research Center program of the National Science Foundation (NSF) under the award number 0313747.

References

Golestani, Y., V. Chandrasekar, and R. Keeler, 1995: Dual polarized staggered prt scheme for weather radars: Analysis and applications. *IEEE Trans. Geoscience and Remote Sensing.*, **33**, 239–246.

Jorgensen, D., T. Shepherd, and A. Goldstein, 2000: A dual-pulse repetition frequency scheme for mitigating velocity ambiguities of the noaa p-3 airborne doppler radar. *J. Atmos. Oceanic Technol.*, **17**, 585–594.

Junyent, F., V. Chandrasekar, D. McLaughlin, S. Frasier, E. Insanic, R. Ahmed, N. Bharadwaj, E. Knapp, L. Krnan, and R. Tessier, 2005: Salientfeatures of radar nodes of the first generation netrad system. *IGARSS'05*, IEEE., 420–423.

Sachidananda, M. and D. Zrnic, 1999: Systematic phas codes for resolving range overlaid signals in a doppler weather radar. *J. Atmos. Oceanic Technol.*, **16**, 1351–1363.

Siggia, A., 1983: Processing phase coded radar signals with adaptive digital filters. *21st Conf. on Radar Meteorology*, Amer. Meteor. Soc., Edmonton, AB, Cannada, 513–518.

Siggia, A. and J. Passarelli, 2004: Gaussian model adaptive processing (gmap) for improved ground clutter cancellation and moment calculation. *European Conference on Radar in Meteorology and Hydrology*, ERAD., 67–73.

Zrnic, D. and P. Mahapatra, 1985: Two methods of ambiguity resolution in pulsed doppler weather radars. *IEEE Trans. Aerosp. Electr. Syst.*, **21**, 470–483.